

Chapter 6

ELECTROSTATIC PRECIPITATORS

James H. Turner
Phil A. Lawless
Toshiaki Yamamoto
David W. Coy
Research Triangle Institute
Research Triangle Park, NC 27709

Gary P. Greiner
John D. McKenna
ETS, Inc.
Roanoke, VA 24018-4394

William M. Vatavuk
Innovative Strategies and Economics Group, OAQPS
U.S. Environmental Protection Agency
Research Triangle Park, NC 27711

December, 1995

Contents

6.1	Process Description	6-5
6.1.1	Introduction	6-5
6.1.2	Types of ESPs	6-5
6.1.2.1	Plate-Wire Precipitators	6-5
6.1.2.2	Flat Plate Precipitators	6-7
6.1.2.3	Tubular Precipitators	6-10
6.1.2.4	Wet Precipitators	6-10
6.1.2.5	Two-Stage Precipitators	6-10
6.1.3	Auxiliary Equipment	6-11
6.1.4	Electrostatic Precipitation Theory	6-12
6.1.4.1	Electrical Operating Point	6-13
6.1.4.2	Particle Charging	6-15
6.1.4.3	Particle Collection	6-18
6.1.4.4	Sneakage and Rapping Reentrainment	6-20
6.2	ESP Design Procedure	6-21
6.2.1	Specific Collecting Area	6-21
6.2.1.1	SCA Procedure with Known Migration Velocity	6-22
6.2.1.2	Full SCA Procedure	6-24
6.2.1.3	Specific Collecting Area for Tubular Precipitators	6-32
6.2.2	Flow Velocity	6-32
6.2.3	Pressure Drop Calculations	6-33

6.2.4	Particle Characteristics	6-36
6.2.5	Gas Characteristics	6-37
6.2.6	Cleaning	6-37
6.2.7	Construction Features	6-38
6.3	Estimating Total Capital Investment	6-39
6.3.1	Equipment Cost	6-39
6.3.1.1	ESP Costs	6-39
6.3.1.2	Retrofit Cost Factor	6-42
6.3.1.3	Auxiliary Equipment	6-43
6.3.1.4	Costs for Two-Stage Precipitators	6-45
6.3.2	Total Purchased Cost	6-45
6.3.3	Total Capital Investment (TCI)	6-46
6.4	Estimating Total Annual Costs	6-46
6.4.1	Direct Annual Costs	6-46
6.4.1.1	Operating and Supervisory Labor	6-46
6.4.1.2	Operating Materials	6-47
6.4.1.3	Maintenance	6-49
6.4.1.4	Electricity	6-49
6.4.1.5	Fuel	6-50
6.4.1.6	Water	6-51
6.4.1.7	Compressed Air	6-51
6.4.1.8	Dust Disposal	6-51
6.4.1.9	Wastewater Treatment	6-51

6.4.1.10 Conditioning Costs	6-52
6.4.2 Indirect Annual Costs	6-52
6.4.3 Recovery Credits	6-52
6.4.4 Total Annual Cost	6-52
6.4.5 Example Problem	6-53
6.4.5.1 Design SCA	6-53
6.4.5.2 ESP Cost	6-57
6.4.5.3 Costs of Auxiliaries	6-57
6.4.5.4 Total Capital Investment	6-57
6.4.5.5 Annual Costs-Pressure Drop	6-58
6.4.5.8 Total Annual Cost	6-61
6.5 Acknowledgments	6-61
Appendix 6A	6-62
References	6-67

6.1 Process Description

6.1.1 Introduction

An electrostatic precipitator (ESP) is a particle control device that uses electrical forces to move the particles out of the flowing gas stream and onto collector plates. The particles are given an electrical charge by forcing them to pass through a corona, a region in which gaseous ions flow. The electrical field that forces the charged particles to the walls comes from electrodes maintained at high voltage in the center of the flow lane.

Once the particles are collected on the plates, they must be removed from the plates without reentraining them into the gas stream. This is usually accomplished by knocking them loose from the plates, allowing the collected layer of particles to slide down into a hopper from which they are evacuated. Some precipitators remove the particles by intermittent or continuous washing with water.

6.1.2 Types of ESPs

ESPs are configured in several ways. Some of these configurations have been developed for special control action, and others have evolved for economic reasons. The types that will be described here are (1) the plate-wire precipitator, the most common variety; (2) the flat plate precipitator, (3) the tubular precipitator; (4) the wet precipitator, which may have any of the previous mechanical configurations; and (5) the two-stage precipitator.

6.1.2.1 Plate-Wire Precipitators

Plate-wire ESPs are used in a wide variety of industrial applications, including coal-fired boilers, cement kilns, solid waste incinerators, paper mill recovery boilers, petroleum refining catalytic cracking units, sinter plants, basic oxygen furnaces, open hearth furnaces, electric arc furnaces, coke oven batteries, and glass furnaces.

In a plate-wire ESP, gas flows between parallel plates of sheet metal and high-voltage electrodes. These electrodes are long wires weighted and hanging between the plates or are supported there by mast-like structures (rigid frames). Within each flow path, gas flow must pass each wire in sequence as flows through the unit.

The plate-wire ESP allows many flow lanes to operate in parallel, and each lane can be quite tall. As a result, this type of precipitator is well suited for handling large volumes of gas. The need for rapping the plates to dislodge the collected material has caused the plate to be divided into sections, often three or four in series with one another, which can be rapped independent. The power supplies are often sectionalized in the same way to obtain higher operating voltages, and further electrical sectionalization may be used for increased reliability. Dust also deposits on the discharge electrode wires and must be periodically removed similarly to the collector plate.

The power supplies for the ESP convert the industrial ac voltage (220 to 480 V) to pulsating dc voltage in the range of 20,000 to 100,000 V as needed. The supply consists of a step-up transformer, high-voltage rectifiers, and sometimes filter capacitors. The unit may supply either half-wave or full-wave rectified dc voltage. There are auxiliary components and controls to allow the voltage to be adjusted to the highest level possible without excessive sparking and to protect the supply and electrodes in the event a heavy arc or short-circuit occurs.

The voltage applied to the electrodes causes the air between the electrodes to break down electrically, an action known as a "corona". The electrodes usually are given a negative polarity because a negative corona supports a higher voltage than a positive corona before sparking occurs. The ions generated in the corona follow electric field lines from the wires to the collecting plates. Therefore, each wire establishes a charging zone through which the particles must pass.

Particles passing through the charging zone intercept some of the ions, which become attached. Small aerosol particles ($<1 \mu\text{m}$ diameter) can absorb tens of ions before their total charge becomes large enough to repel further ions, and large particles ($>10 \mu\text{m}$ diameter) can absorb tens of thousands. The electrical forces are therefore much stronger on the large particles.

As the particles pass each successive wire, they are driven closer and closer to the collecting walls. The turbulence in the gas, however, tends to keep them uniformly mixed with the gas. The collection process is therefore a competition between the electrical and dispersive forces. Eventually, the particles approach close enough to the walls so that the turbulence drops to low levels and the particles are collected.

If the collected particles could be dislodged into the hopper without losses, the ESP would be extremely efficient. The rapping that dislodges the accumulated layer also projects some of the particles (typically 12 percent for coal fly ash) back into the gas stream. These reentrained particles are then processed again by later sections, but the particles reentrained in the last section of the ESP have no chance to be recaptured and so escape the unit.

Practical considerations of passing the high voltage into the space between the lanes and allowing for some clearance above the hoppers to support and align electrodes leave room for part of the gas to flow around the charging zones. This is called "sneakage" and amounts to 5 to 10 percent of the total flow. Antisneakage baffles usually are placed to force the sneakage flow to mix with the main gas stream for collection in later sections. But, again, the sneakage flow around the last section has no opportunity to be collected.

These losses play a significant role in the overall performance of an ESP. Another major factor is the resistivity of the collected material. Because the particles form a continuous layer on the ESP plates, all the ion current must pass through the layer to reach the ground-plates. This current creates an electric field in the layer, and it can become large enough to cause local electrical breakdown. When this occurs, new ions of the wrong polarity are injected into the wire-plate gap where they reduce the charge on the particles and may cause sparking. This breakdown condition is called "back corona"

Back corona is prevalent when the resistivity of the layer is high, usually above 2×10^{11} ohm-cm. For lower resistivities, the operation of the ESP is not impaired by back coronas, but resistivities much higher than 2×10^{11} ohm-cm considerably reduce the collection ability of the unit because the severe back corona causes difficulties in charging the particles. At resistivities below 10^8 ohm-cm, the particles are held on the plates so loosely that rapping and nonrapping reentrainment become much more severe. Care must be taken in measuring or estimating resistivity because it is strongly affected by variables such as temperature, moisture, gas composition, particle composition, and surface characteristics.

6.1.2.2 Flat Plate Precipitators

A significant number of smaller precipitators (100,000 to 200,000 acfm) use flat plates instead of wires for the high-voltage electrodes. The flat plates (United McGill Corporation patents) increase the average electric field that can be used to collect the particles, and they provide an increased surface area for the collection of particles. Corona cannot be generated on flat plates by themselves, so corona-generating electrodes are placed ahead of and sometimes behind the flat plate collecting zones. These electrodes may be sharp-pointed needles attached to the edges of the plates or independent corona wires. Unlike plate-wire or tubular ESPs, this design operates equally well with either negative or positive polarity. The manufacturer has chosen to use positive polarity to reduce ozone generation.

A flat plate ESP operates with little or no corona current flowing through the collected dust, except directly under the corona needles or wires. This has two consequences. The first is that the unit is somewhat less susceptible to back corona than conventional units are because no back corona is generated in the collected dust, and particles charged with both polarities of ions have large collection surfaces available. The second consequence is that the lack of current in the collected layer causes an electrical force that tends to remove the layer from the collecting surface; this can lead to high rapping losses.

Flat plate ESPs seem to have wide application for high-resistivity particles with small (1 to $2 \mu\text{m}$) mass median diameters (MMDs). These applications especially emphasize the strengths of the design because the electrical dislodging forces are weaker for small particles than for large ones. Fly ash has been successfully collected with this type of ESP, but low-flow velocity appears to be critical for avoiding high rapping losses.

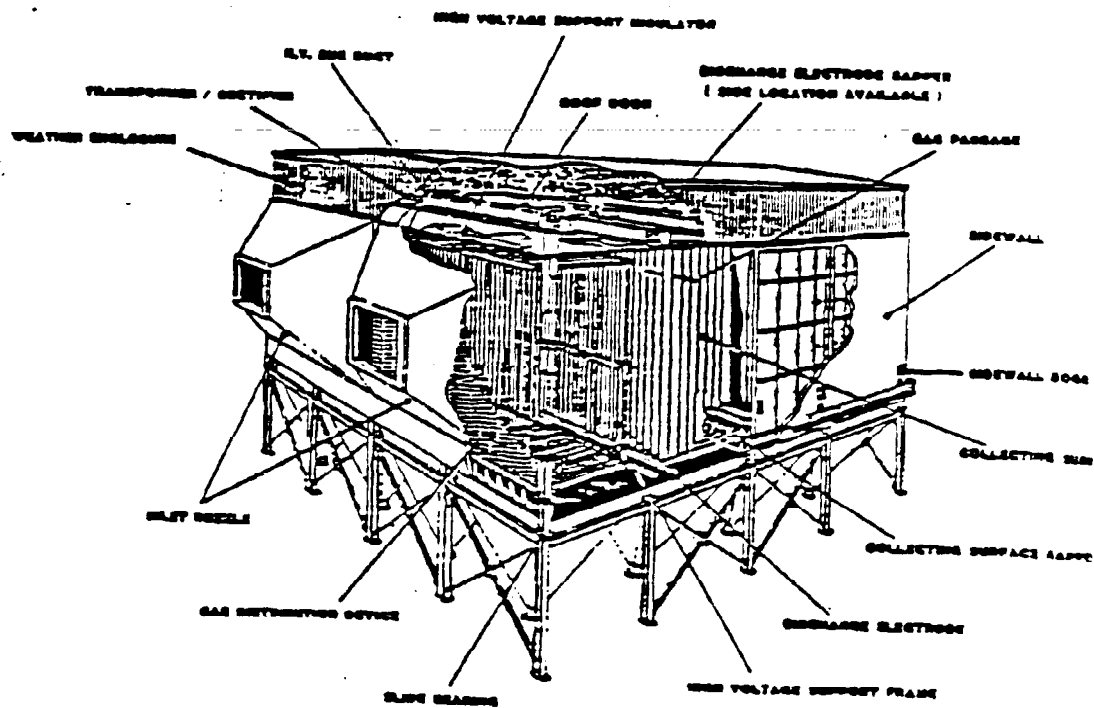


Figure 6.1: Electrostatic Precipitator Components
 (Courtesy of the Institute for Clean Air Companies)

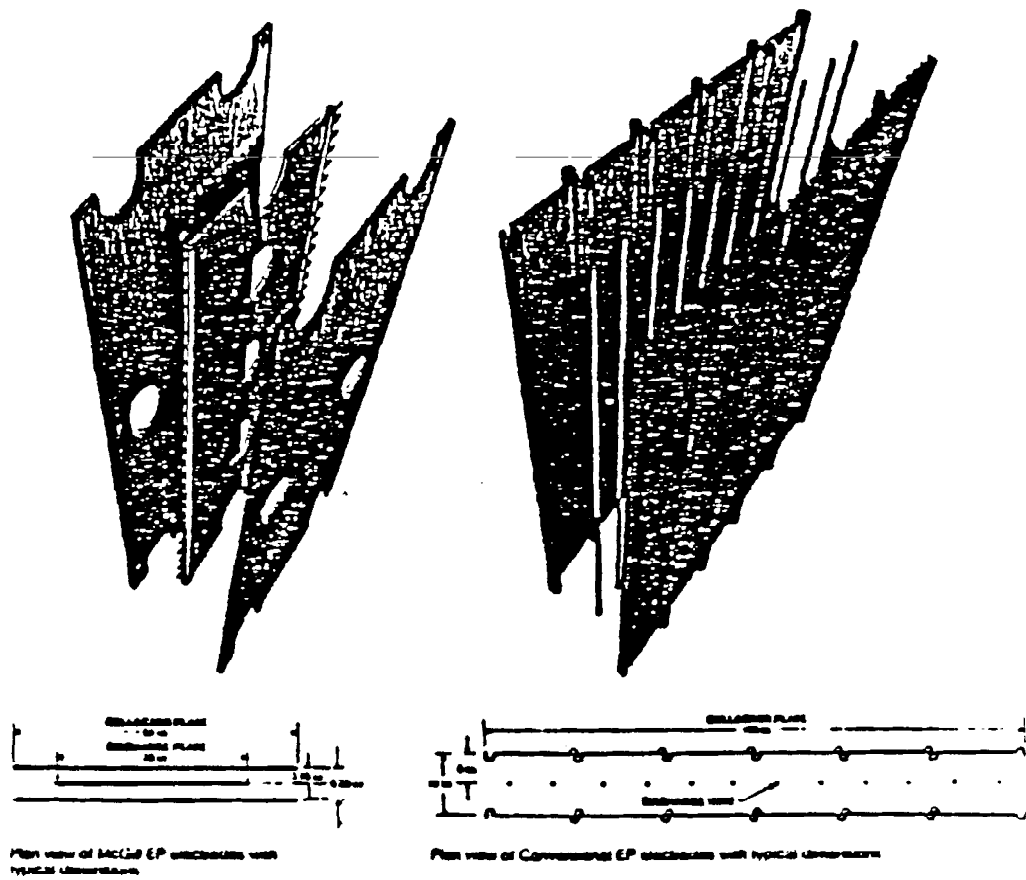


Figure 6.2: Flat-plate and Plate-wire ESP Configurations
(Courtesy of United McGill Corporation)

6.1.2.3 Tubular Precipitators

The original ESPs were tubular like the smokestacks they were placed on, with the high-voltage electrode running along the axis of the tube. Tubular precipitators have typical applications in sulfuric acid plants, coke oven by-product gas cleaning (tar removal), and, recently, iron and steel sinter plants. Such tubular units are still used for some applications, with many tubes operating in parallel to handle increased gas flows. The tubes may be formed as a circular, square, or hexagonal honeycomb with gas flowing upwards or downwards. The length of the tubes can be selected to fit conditions. A tubular ESP can be tightly sealed to prevent leaks of material, especially valuable or hazardous material.

A tubular ESP is essentially a one-stage unit and is unique in having all the gas pass through the electrode region. The high-voltage electrode operates at one voltage for the entire length of the tube, and the current varies along the length as the particles are removed from the system. No sneakage paths are around the collecting region, but corona nonuniformities may allow some particles to avoid charging for a considerable fraction of the tube length.

Tubular ESPs comprise only a small portion of the ESP population and are most commonly applied where the particulate is either wet or sticky. These ESPs, usually cleaned with water, have reentrainment losses of a lower magnitude than do the dry particulate precipitators.

6.1.2.4 Wet Precipitators

Any of the precipitator configurations discussed above may be operated with wet walls instead of dry. The water flow may be applied intermittently or continuously to wash the collected particles into a sump for disposal. The advantage of the wet wall precipitator is that it has no problems with rapping reentrainment or with back coronas. The disadvantage is the increased complexity of the wash and the fact that the collected slurry must be handled more carefully than a dry product, adding to the expense of disposal.

6.1.2.5 Two-Stage Precipitators

The previously described precipitators are all parallel in nature, *i.e.*, the discharge and collecting electrodes are side by side. The two-stage precipitator invented by Penney is a series device with the discharge electrode, or ionizer, preceding the collector electrodes. For indoor applications, the unit is operated with positive polarity to limit ozone generation.

Advantages of this configuration include more time for particle charging, less propensity for back corona, and economical construction for small sizes. This type of precipitator is generally used for gas flow volumes of 50,000 acfm and less and is applied to submicrometer sources

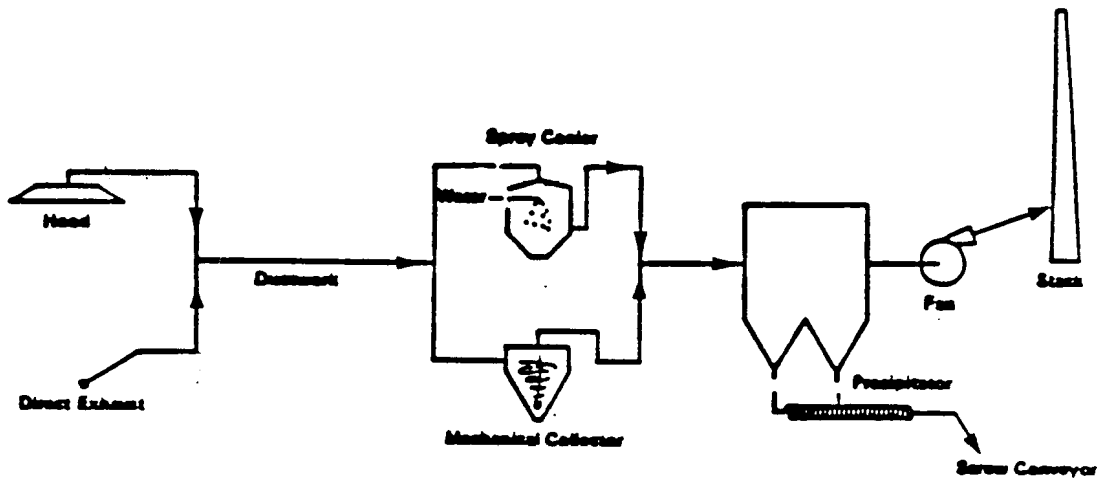


Figure 6.3: Control Device and Typical Auxiliary Equipment

emitting oil mists, smokes, fumes, or other sticky particulates because there is little electrical force to hold the collected particulates on the plates. Modules consisting of a mechanical prefilter, ionizer, collecting-plate cell, after-filter, and power pack may be placed in parallel or series-parallel arrangements. Preconditioning of gases is normally part of the system. Cleaning may be by water wash of modules removed from the system up to automatic, in-place detergent spraying of the collector followed by air-blow drying.

Two-stage precipitators are considered to be separate and distinct types of devices compared to large, high-gas-volume, single-stage ESPs. The smaller devices are usually sold as pre-engineered, package systems.

6.1.3 Auxiliary Equipment

Typical auxiliary equipment associated with an ESP system is shown schematically in Figure 6.3. Along with the ESP itself, a control system usually includes the following auxiliary equipment: a capture device (*i.e.*, hood or direct exhaust connection); ductwork; dust removal equipment (screw conveyor, etc.); fans, motors, and starters; and a stack. In addition, spray coolers and mechanical collectors may, be needed to precondition the gas before it reaches the ESP. Capture devices are usually hoods that exhaust pollutants into the ductwork or are direct exhaust couplings attached to a combustor or process equipment. These devices are usually refractory lined, water cooled, or simply fabricated from carbon steel, depending on the gas-stream temperatures. Refractory or water-cooled capture devices are used where the wall temperatures exceed 800°F; carbon steel is used for lower temperatures. The ducting, like the capture device, should be water cooled, refractory, or stainless steel for hot processes and carbon steel for gas temperatures below approximately 1,150°F (duct wall temperatures <800°F). The ducts should be sized for a gas velocity of approximately 4,000 ft/min for the average case to prevent particle deposition in the ducts. Large or dense particles might require higher velocities,

but rarely would lower velocities be used. Spray chambers may be required for processes where the addition of moisture, or decreased temperature or gas volume, will improve precipitation or protect the ESP from warpage. For combustion processes with exhaust gas temperatures below approximately 700°F, cooling would not be required, and the exhaust gases can be delivered directly to the precipitator.

When much of the pollutant loading consists of relatively large particles, mechanical collectors, such as cyclones, may be used to reduce the load on the ESP, especially at high inlet concentrations. The fans provide the motive power for air movement and can be mounted before or after the ESP. A stack, normally used, vents the cleaned stream to the atmosphere. Screw conveyors or pneumatic systems are often used to remove captured dust from the bottom of the hoppers.

Wet ESPs require a source of wash water to be injected or sprayed near the top of the collector plates either continuously or at timed intervals. The water flows with the collected particles into a sump from which the fluid is pumped. A portion of the fluid may be recycled to reduce the total amount of water required. The remainder is pumped directly to a settling pond or passed through a dewatering stage, with subsequent disposal of the sludge.

Gas conditioning equipment to improve ESP performance by changing dust resistivity is occasionally used as part of the original design, but more frequently it is used to upgrade existing ESPs. The equipment injects an agent into the gas stream ahead of the ESP. Usually, the agent mixes with the particles and alters their resistivity to promote higher migration velocity, and thus higher collection efficiency. However, electrical properties of the gas may change, rather than dust resistivity. For instance, cooling the gas will allow more voltage to be applied before sparking occurs. Significant conditioning agents that are used include SO_3 , H_2SO_4 , sodium compounds, ammonia, and water, but the major conditioning agent by usage is SO_3 . A typical dose rate for any of the gaseous agents is 10 to 30 ppm by volume.

The equipment required for conditioning depends on the agent being used. A typical SO_3 conditioner requires a supply of molten sulfur. It is stored in a heated vessel and supplied to a burner, where it is oxidized to SO_2 . The SO_2 gas is passed over a catalyst for further oxidation to SO_3 . The SO_3 gas is then injected into the flue gas stream through a multi-outlet set of probes that breach a duct. In place of a sulfur burner to provide SO_2 , liquid SO_2 may be vaporized from a storage tank. Although their total annual costs are higher, the liquid SO_2 systems have lower capital costs and are easier to operate than the molten sulfur based systems.

Water or ammonia injection requires a set of spray nozzles in the duct, along with pumping and control equipment.

Sodium conditioning is often done by coating the coal on a conveyor with a powder compound or a water solution of the desired compound. A hopper or storage tank is often positioned over the conveyor for this purpose.

6.1.4 Electrostatic Precipitation Theory

The theory of ESP operation requires many scientific disciplines to describe it thoroughly. The ESP is basically an electrical machine. The principal actions are the charging of particles and forcing them to the collector plates. The amount of charged particulate matter affects the electrical operating point of the ESP. The transport of the particles is affected by the level of turbulence in the gas. The losses mentioned earlier, sneakage and rapping reentrainment, are major influences on the total performance of the system. The particle properties also leave a major effect on the operation of the unit.

The following subsections will explain the theory behind (1) electrical operating points in the ESP, (2) particle charging, (3) particle collection, and (4) sneakage and rapping reentrainment. General references for these topics are White [1] or Lawless and Sparks [2].

6.1.4.1 Electrical Operating Point

The electrical operating point of an ESP section is the value of voltage and current at which the section operates. As will become apparent, the best collection occurs when the highest electric field is present, which roughly corresponds to the highest voltage on the electrodes. In this work, the term "section" represents one set of plates and electrodes in the direction of flow. This unit is commonly called a "field", and a "section" or "bus section" represents a subdivision of a "field" perpendicular to the direction of flow. In an ESP model and in sizing applications, the two terms "section" and "field" are used equivalently because the subdivision into bus sections should have no effect on the model. This terminology has probably arisen because of the frequent use of the word "field" to refer to the electric field.

The lowest acceptable voltage is the voltage required for the formation of a corona, the electrical discharge that produces ions for charging particles. The (negative) corona is produced when an occasional free electron near the high-voltage electrode, produced by a cosmic ray, gains enough energy from the electric field to ionize the gas and produce more free electrons. The electric field for which this process is self-sustained has been determined experimentally. For round wires, the field at the surface of the wire is given by:

$$E_c = 3.126 \times 10^6 d_r [1 + 0.0301 (d_r / r_w)^{0.5}] \quad (6.1)$$

where

- E_c = corona onset field *at the wire surface* (V/m)
- d_r = relative gas density, referred to 1 atm pressure and 20°C (dimensionless)
- r_w = radius of the wire, meters (m)

This is the field required to produce "glow" corona, the form usually seen in the laboratory on smooth, clean wires. The glow appears as a uniform, rapidly moving diffuse light around the electrode. After a period of operation, the movement concentrates into small spots on the wire surface, and the corona assumes a tuft-like appearance. The field required to produce "tuft" corona, the form found in full-scale ESPs, is 0.6 times the value of E_c .

The voltage that must be applied to the wire to obtain this value of field, V_c , is found by integrating the electric field from the wire to the plate. The field follows a simple "1/r" dependence in cylindrical geometry. This leads to a logarithmic dependence of voltage on electrode dimensions. In the plate-wire geometry, the field dependence is somewhat more complex, but the voltage still shows the logarithmic dependence. V_c is given by:

$$V_c = E_c r_w \ln \left(\frac{d}{r_w} \right) \quad (6.2)$$

where

- V_c = corona onset voltage (V)
- d = outer cylinder radius for tubular ESP (m)
4/ x (wire-plate separation) for plate-wire ESP (m)

No current will flow until the voltage reaches this value, but the amount of current will increase steeply for voltages above this value. The maximum current density (amperes/square meter) on the plate or cylinder directly under the wire is given by:

$$j = \mu \epsilon \frac{V^2}{L^3} \quad (6.3)$$

where

- j = maximum current density (A/m^2)
- μ = ion mobility m^2/Vs (meter²/volt second)
- = free space permittivity (8.845×10^{-12} F/m)(Farad/meter)
- V = applied voltage (V)
- L = shortest distance from wire to collecting surface (m)

For tuft corona, the current density is zero until the corona onset voltage is reached, when it jumps almost to this value of j within a few hundred volts, directly under a tuft.

The region near the wire is strongly influenced by the presence of ions there, and the corona onset voltage magnitude shows strong spatial variations. Outside the corona region, it is quite uniform.

The electric field is strongest along the line from wire to plate and is approximated very well, except near the wire, by:

$$E_{max} = V / L \quad (6.4)$$

where

$$E_{max} = \text{maximum field strength (V/m)}$$

When the electric field throughout the gap between the wire and the plate becomes strong enough, a spark will occur, and the voltage cannot be increased without severe sparking occurring. The field at which sparking occurs is not sharply defined, but a reasonable value is given by:

$$E_s = 6.3 \times 10^5 \left(\frac{273}{T} P \right)^{1.65} \quad (6.5)$$

where

$$\begin{aligned} E_s &= \text{sparking field strength (V/m)} \\ T &= \text{absolute temperature (K)} \\ P &= \text{gas pressure (atm)} \end{aligned}$$

This field would be reached at a voltage of, for example, 35,000 V for a plate-wire spacing of 11.4 cm (4.5 in.) at a temperature of 149°C (300°F). The ESP will generally operate near this voltage in the absence of back corona. E_{max} will be equal to or less than E_s .

Instead of sparking, back corona may occur if the electric field in the dust layer, resulting from the current flow in the layer, reaches a critical value of about 1×10^6 V/m. Depending on conditions, the back corona, may enhance sparking or may generate so much current that the voltage cannot be raised any higher. The field in the layer is given by:

$$E_l = j\tilde{\rho}$$

where

$$\begin{aligned} E_l &= \text{electric field in dust layer (V/m)} \\ &= \text{resistivity of the collected material (ohm-m)} \end{aligned}$$

6.1.4.2 Particle Charging

Charging of particles takes place when ions bombard the surface of a particle. Once an ion is close to the particle, it is tightly bound because of the image charge within the particle. The "image charge" is a representation of the charge distortion that occurs when a real charge approaches a conducting surface. The distortion is equivalent to a charge of opposite magnitude to the real charge, located as far below the surface as the real charge is above it. The notion of the fictitious charge is similar to the notion of an image in a mirror, hence the name. As more ions accumulate on a particle, the total charge tends to prevent further ionic bombardment.

There are two principal charging mechanisms: diffusion charging and field charging. Diffusion charging results from the thermal kinetic energy of the ions overcoming the repulsion of the ions already on the particle. Field charging occurs when ions follow electric field lines until they terminate on a particle. In general, both mechanisms are operative for all sizes of particles. Field charging, however, adds a larger percentage of charge on particles greater than about $2\mu\text{m}$ in diameter, and diffusion charging adds a greater percentage on particles smaller than about $0.5\mu\text{m}$.

Diffusion charging, as derived by White [1], produces a logarithmically increasing level of charge on particles, given by:

$$q(t) = \left(\frac{rkT}{e} \right) \ln(1 + r)$$

where

- $q(t)$ = particle charge (C) as function of time, t, in seconds
- r = particle radius (m)
- k = Boltzmann's constant (j/K)
- T = absolute temperature (K)
- e = electron charge ($1.67 \times 10^{-19} \text{C}$)
- = dimensionless time given by:

$$\hat{\theta} = \frac{\delta r v N e^2 \hat{e}}{kT} \tag{6.8}$$

where

- v = mean thermal speed of the ions (m/s)
- N = ion number concentration near the particle (No./m^3) = real time (exposure
- θ = real time (exposure time in the charging zone) (s)

Diffusion charging never reaches a limit, but it becomes very slow after about three dimensionless time units. For fixed exposure times, the charge on a particle is proportional to its radius.

Field charging also exhibits a characteristic time-dependence, given by:

$$q(t) = q_s \tau / (\tau + t) \quad (6.9)$$

where

- q_s = saturation charge, charge at infinite time (C)
- τ = real time (s)
- t = another dimensionless time unit

The saturation charge is given by:

$$q_s = 12\pi\epsilon_0 r^2 E \quad (6.10)$$

where

- ϵ_0 = free space permittivity (F/m)
- E = external electric field applied to the particle (V/m)

The saturation charge is proportional to the square of the radius, which explains why field charging is the dominant mechanism for larger particles. The field charging time constant is given by:

$$\tau = 4\pi\epsilon_0 r^2 / Ne\mu \quad (6.11)$$

where

- μ = ion mobility

Strictly speaking, both diffusion and field charging mechanisms operate at the same time on all particles, and neither mechanism is sufficient to explain the charges measured on the particles. It has been found empirically that a very good approximation to the measured charge is given by the sum of the charges predicted by equations 6.7 and 6.9 independently of one another:

$$q_{tot} = q_d(t) + q_f(t) \quad (6.12)$$

where

- $q_{tot}(t)$ = particle charge due to both mechanisms
- $q_d(t)$ = particle charge due to diffusion charging
- $q_f(t)$ = particle charge due to field charging

6.1.4.3 Particle Collection

The electric field in the collecting zone produces a force on a particle proportional to the magnitude of the field and to the charge:

$$F_e = qE \quad (6.13)$$

where

- F_e = force due to electric field (N)
- q = charge on particle (C)
- E = electric field (V/m)

Because the field charging mechanism gives an ultimate charge proportional to the electric field, the force on large particles is proportional to the square of the field, which shows the advantage for maintaining as high a field as possible.

The motion of the particles under the influence of the electric field is opposed by the viscous drag of the gas. By equating the electric force and the drag force component due to the electric field (according to Stokes' law), we can obtain the particle velocity:

$$v(q, E, r) = \frac{q(E, r) \times E \times C(r)}{6\delta\zeta r} \quad (6.14)$$

where

- $v(q, E, r)$ = particle velocity (m/s)
- $q(E, r)$ = particle charge (C)
- $C(r)$ = Cunningham correction to Stokes' law (dimensionless)
- = gas viscosity (kg/ms)

The particle velocity, is the rate at which the particle moves along the electric field lines, *i.e.*, toward the walls.

For a given electric field, this velocity is usually at a minimum for particles of about $0.5 \mu\text{m}$ diameter. Smaller particles move faster because the charge does not decrease very much, but the

Cunningham factor increases rapidly as radius decreases. Larger particles have a charge increasing as r^2 and a viscous drag only increasing as r^1 ; the velocity then increases as r .

Equation 6.14 gives the particle velocity with respect to still air. In the ESP, the flow is usually very turbulent, with instantaneous gas velocities of the same magnitude as the particles velocities, but in random directions. The motion of particles toward the collecting plates is therefore a statistical process, with an average component imparted by the electric field and a fluctuating component from the gas turbulence.

This statistical motion leads to an exponential collection equation, given by:

$$N(r) = N_0(r) \times \exp(-v(r) / v_0) \quad (6.15)$$

where

- $N(r)$ = particle concentration of size r at the exit of the collecting zone (No./m³)
- $N_0(r)$ = particle concentration of size r at the entrance of the zone (No./m³)
- $v(r)$ = size-dependent particle velocity (m/s)
- v_0 = characteristic velocity of the ESP (m/s), given by:

$$v_0 = Q / A = 1 / SCA \quad (6.16)$$

where

- Q = volume flow rate of the gas (m³/s)
- A = plate area for the ESP collecting zone (m²)
- SCA = specific collection area (A/Q) (s/m)

When this collection equation is averaged over all the particle sizes and weighted according to the concentration of each size, the Deutsch equation results, with the penetration (fraction of particles escaping) given by:

$$p = \exp(-w_e \times SCA) \quad (6.17)$$

where

- p = penetration (fraction)
- w_e = effective migration velocity for the particle ensemble (m/s)

The efficiency is given by:

$$\text{Eff} (\%) = 100 (1 - p) \quad (6.18)$$

and is the number most often used to describe the performance of an ESP.

6.1.4.4 Sneakage and Rapping Reentrainment

Sneakage and rapping reentrainment are best considered on the basis of the sections within an ESP. Sneakage occurs when a part of the gas flow bypasses the collection zone of a section. Generally, the portion of gas that bypasses the zone is thoroughly mixed with the gas that passes through the zone before all the gas enters the next section. This mixing cannot always be assumed, and when sneakage paths exist around several sections, the performance of the whole ESP is seriously effected. To describe the effects of sneakage and rapping reentrainment mathematically we first consider sneakage by itself and then consider the effects of rapping as an average over many rapping cycles.

On the assumption that the gas is well mixed between sections, the penetration for each section can be expressed as:

$$p_s = S_N + [(1 - S_N) \times p_c(Q')] \quad (6.19)$$

where

- p_s = section's fractional penetration
- S_N = fraction of gas bypassing the section (sneakage)
- $p_c(Q)$ = fraction of particles penetrating the collection zone, which is functionally dependent on Q , the gas volume flow in the collection zone, reduced by the sneakage (m^3/s)

The penetration of the entire ESP is the product of the section penetrations. The sneakage sets a lower limit on the penetration of particles through the section.

To calculate the effects of rapping, we first calculate the amount of material captured on the plates of the section. The fraction of material that was caught is given by:

$$m/m_o = 1 - p_s = 1 - S_N - [(1 - S_N) \times p_c(Q')] \quad (6.20)$$

where

- m/m_o = mass fraction collected from the gas stream

This material accumulates until the plates are rapped, whereupon most of the material falls into the hopper for disposal, but a fraction of it is reentrained and leaves the section. Experimental measurements have been conducted on fly ash ESPs to evaluate the fraction reentrained, which averages about 12 percent.

The average penetration for a section including sneakage and rapping reentrainments, is:

$$S_N + [(1 - S_N) \times p_c(Q')] + RR(1 - S_N)[1 - p_c(Q')] \quad (6.21)$$

where

RR = fraction reentrained

This can be written in a more compact form as:

$$p_s = LF + [(1 - LF) \times p_c(Q')] \quad (6.22)$$

by substituting LF (loss factor) for $S_N + RR(1 - S_N)$. These formulas can allow for variable amounts of sneakage and rapping reentrainment for each section, but there is no experimental evidence to suggest that it is necessary.

Fly ash precipitators analyzed in this way have an average S_N of 0.07 and an RR of 0.12. These values are the best available at this time, but some wet ESPs, which presumably have no rapping losses, have shown S_N values of 0.05 or less. These values offer a means for estimating the performance of ESPs whose actual characteristics are not known, but about which general statements can be made. For instance, wet ESPs would be expected to have $RR = 0$, as would ESPs collecting wet or sticky particles. Particulate materials with a much smaller mass mean diameter, MMD , than fly ash would be expected to have a lower RR factor because they are held more tightly to the plates and each other. Sneakage factors are harder to account for; unless special efforts have been made in the design to control sneakage, the 0.07 value should be used.

6.2 ESP Design Procedure

6.2.1 Specific Collecting Area

Specific collecting area (SCA) is a parameter used to compare ESPs and roughly estimate their collection efficiency. SCA is the total collector plate, area divided by gas volume flow rate and has the units of s/m or s/ft . Since SCA is the ratio of A/Q , it is often expressed as $m^2/(m^3/s)$ or $ft^2/kacfm$, where $kacfm$ is thousand $acfm$. SCA is also one of the most important factors in determining the capital and several of the annual costs (for example, maintenance and dust

disposal costs) of the ESP because it determines the size of the unit. Because of the various ways in which SCA can be expressed, Table 6.1 gives equivalent SCAs in the different units for what would be considered a small, medium, and large SCA.

Table 6.1: Small, Medium, and Large SCAs as Expressed by Various Units

Units	Small	Medium	Large
ft ² /kacfm	100	400	900
s/m	19.7	78.8	177
s/ft	6	24	54

5.080 ft²/kacfm = 1 (s/m).

The design procedure is based on the loss factor approach of Lawless and Sparks [2] and considers a number of process parameters. It can be calculated by hand, but it is most conveniently used with a spreadsheet program. For many uses, tables of effective migration velocities can be used to obtain the SCA required for a given efficiency. In the following subsection, tables have been calculated using the design procedure for a number of different particle sources and for differing levels of efficiency. If a situation is encountered that is not

covered in these tables, then the full procedure that appears in the subsequent subsection should be used.

6.2.1.1 SCA Procedure with Known Migration Velocity

If the migration velocity is known, then equation 6.17 can be rearranged to give the SCA:

$$SCA = -\ln(p) / w_e \quad (6.23)$$

A graphical solution to equation 6.23 is given in Figure 6.4. The migration velocities have been calculated for three main precipitator types: plate-wire, flat plate, and wet wall ESPs of the plate-wire type. The following three tables, keyed to design efficiency as an easily quantified variable, summarize the migration velocities under various conditions:

- In Table 6.2, the migration velocities are given for a plate-wire ESP with conditions of no back corona and severe back corona; temperatures appropriate for each process have been assumed.
- In Table 6.3, the migration velocities calculated for a wet wall ESP of the plate-wire type assume no back corona and no rapping reentrainment.

- In Table 6.4, the flat plate ESP migration velocities are given only for no back corona conditions because they appear to be less affected by high-resistivity dusts than the plate-wire types.

It is generally expected from experience that the migration velocity will decrease with increasing efficiency. In Tables 6.2 through 6.4, however, the migration velocities show some fluctuations. This is because the number of sections must be increased as the efficiency increases, and the changing sectionalization affects the overall migration velocity. This effect is particularly noticeable, for example, in Table 6.4 for glass plants. When the migration velocities in the tables are used to obtain SCAs for the different efficiencies in the tables, the SCAs will increase as the efficiency increases.

6.2.1.2 Full SCA Procedure

The full procedure for determining the SCA for large plate-wire, flat plate, and (with restrictions) tubular dry ESPs is given here. This procedure does not apply to the smaller, two-stage precipitators because these are packaged modules generally sized and sold on the basis of the waste gas volumetric flow rate. Nor does this procedure apply to determining the SCA for wet ESPs. The full procedure consists of the 15 steps given below:

Step 1 – Determine the design efficiency, Eff (%). Efficiency is the most commonly used term in the industry and is the reference value for guarantees however, if it has not been specified, it can be computed as follows:

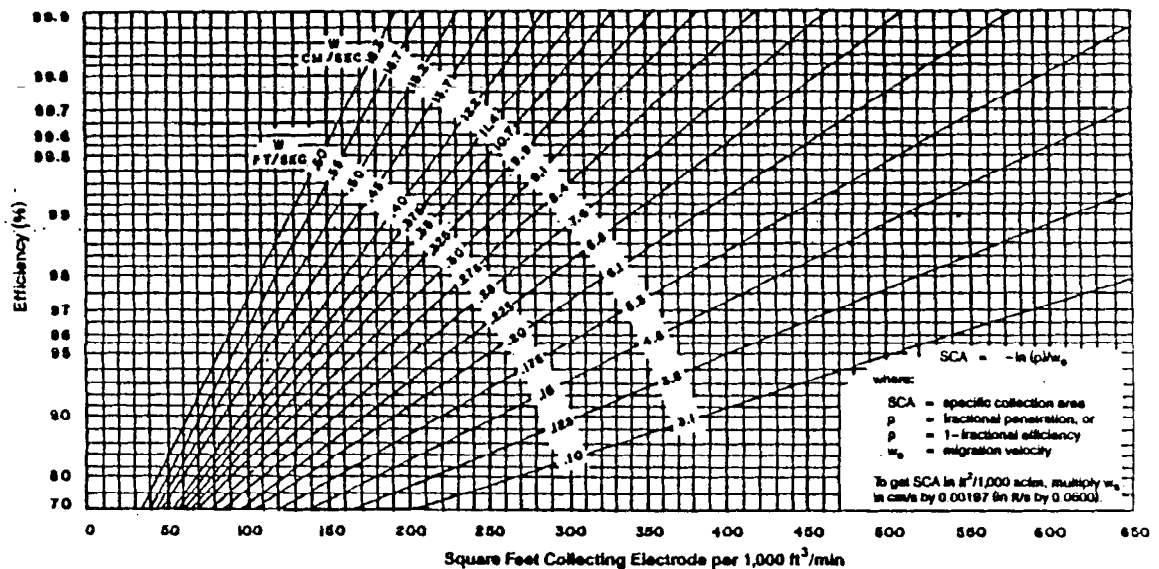


Figure 6.4: Chart for Finding SCA

$$\text{Eff}(\%) = 100 \times (1 - \text{outlet load/inlet load})$$

Step 2 – Compute design penetration, p :

$$p = 1 - (\text{Eff}/100)$$

Step 3 – Compute or obtain the operating temperature, T_k , K. Temperature in Kelvin is required in the calculations which follow.

Table 6.2: Plate-wire ESP Migration Velocities
(cm/s)^a

Particle Source		Design Efficiency, %			
		95	99	99.5	99.9
Bituminous coal fly ash ^b	(no BC)	12.6	10.1	9.3	8.2
	(BC)	3.1	2.5	2.4	2.1
Sub-bituminous coal fly ash in tangential-fired boiler ^b	(no BC)	17.0	11.8	10.3	8.8
	(BC)	4.9	3.1	2.6	2.2
Other coal ^b	(no BC)	9.7	7.9	7.9	7.2
	(BC)	2.9	2.2	2.1	1.9
Cement kiln ^c	(no BC)	1.5	1.5	1.8	1.8
	(BC)	0.6	0.6	0.5	0.5
Glass plant ^d	(no BC)	1.6	1.6	1.5	1.5
	(BC)	0.5	0.5	0.5	0.5
Iron/steel sinter plant dust with mechanical precollector ^b	(no BC)	6.8	6.2	6.6	6.3
	(BC)	2.2	1.8	1.8	1.7
Kraft-paper recovery boiler ^b	(no BC)	2.6	2.5	3.1	2.9
Incinerator fly ash ^e	(no BC)	15.3	11.4	10.6	9.4
Copper reverberatory furnace ^f	(no BC)	6.2	4.2	3.7	2.9
Copper converter ^g	(no BC)	5.5	4.4	4.1	3.6
Copper roaster ^h	(no BC)	6.2	5.5	5.2	4.3
Coke plant combustion stack ⁱ	(no BC)	1.2 ^j	—	—	—

BC = Back corona.

^aTo convert cm/s to ft/s, multiply cm/s by 0.0328. Computational procedure uses SI units, to convert cm/s to m/s, multiply cm/s by 0.01. Assumes same particle size as given in full computational procedure.

^bAt 300°F. Depending on individual furnace/boiler conditions, chemical nature of the fly ash, and availability of naturally occurring conditioning agents (e.g., moisture in the gas stream), migration velocities may vary considerably from these values. Likely values are in the range from back corona to no back corona.

^cAt 600°F. ^dAt 300°F. ^eAt 250°F. / 450 to 570 °F.

^f500 to 700 °F. ^g600 to 660 °F. ^h360 to 450 °F.

ⁱData available only for inlet concentrations in the range of 0.02 to 0.2 g/s m³ and for efficiencies less than 90 percent.

Table 6.3: Wet Wall Plate-wire ESP Migration Velocities
(No back corona, cm/s)^a

Particle Source ^b	Design Efficiency, %			
	95	99	99.5	99.9
Bituminous coal fly ash	31.4	33.0	33.8	24.9
Sub-bituminous coal fly ash in tangential-fired boiler	40.0	42.7	44.1	31.4
Other coal	21.1	21.4	21.5	17.0
Cement kiln	6.4	5.6	5.0	5.7
Glass plant	4.6	4.5	4.3	3.8
Iron/steel sinter plant dust with mechanical precollector	14.0	13.7	13.3	11.6

^aTo convert cm/s to ft/s, multiply cm/s by 0.0328. Computational procedure uses SI units; to convert cm/s to m/s, multiply cm/s by 0.01. Assumes same particle size as given in full computational procedure.

^bAll sources assumed at 200 °F.

Table 6.4: Flat Plate ESP Migration Velocities^a
(No back corona, cm/s)^b

Particle Source	Design Efficiency, %			
	95	99	99.5	99.9
Bituminous coal fly ash ^c	13.2	15.1	18.6	16.0
Sub-bituminous coal fly ash in tangential-fired boiler ^c	28.6	18.2	21.2	17.7
Other coal ^c	15.5	11.2	15.1	13.5
Cement kiln ^d	2.4	2.3	3.2	3.1
Glass plant ^e	1.8	1.9	2.6	2.6
Iron/steel sinter plant dust with mechanical precollector ^c	13.4	12.1	13.1	12.4
Kraft-paper recovery boiler ^c	5.0	4.7	6.1	5.8
Incinerator fly ash ^f	25.2	16.9	21.1	18.3

^aAssumes same particle size as given in full computational procedure. These values give the grounded collector plate SCA, from which the collector plate area is derived. In flat plate ESPs, the discharge or high-voltage plate area is typically 40 percent of the ground-plate area. The flat-plate manufacturer usually counts all the plate area (collector plates plus discharge plates) in meeting an SCA specification, which means that the velocities tabulated above must be divided by 1.4 to be used on the manufacturer's basis.

^bTo convert cm/s to ft/s, multiply cm/s by 0.0328. Computational procedure uses SI units; to convert cm/s to m/s, multiply cm/s by 0.01.

^cAt 300° F.

^dAt 600° F.

^eAt 500° F.

^fAt 250° F.

Step 4 – Determine whether severe back corona is present. Severe back corona usually occurs for dust resistivities above 2×10^{11} ohm-cm. Its presence will greatly increase the size of the ESP required to achieve a certain efficiency.

Step 5 – Determine the MMD of the inlet particle distribution MMD_i (μm). If this is not known, assume a value from the following table:

Source	MMD_i (μm)
Bituminous coal	16
Subbituminous coal, tangential boiler	21
Sub-bituminous coal, other boiler types	10 to 15
Cement kiln	2 to 5
Glass plant	1
Wood burning boiler	5
Sinter plant, with mechanical precollector	50 6
	2
Kraft Process Recovery	15 to 30
Incinerators	1
Copper reverberatory furnace	1
Copper converter	1
Coke plant combustion stack	1
Unknown	

Step 6 - Assume value for sneakage, S_N , and rapping reentrainment, RR , from the following tables:

ESP Type	S_N
Plate-wire	0.07
Wet wall	0.05
Flat plate	0.10

ESP / Ash Type	RR
Coal fly ash, or not known	0.14
Wet Wall	0.0
Flat plate with gas velocity > 1.5 m/s (not glass or cement)	0.15
Glass or cement	0.10

Step 7 – Assume values for the most penetrating size, MMD_p , and rapping puff size, MMD_r :

$$\begin{aligned} \text{MMD}_p &= 2 \mu\text{m} \\ \text{MMD}_r &= 5 \mu\text{m} \text{ for ash with } \text{MMD}_i > 5 \mu\text{m} \\ \text{MMD}_r &= 3 \mu\text{m} \text{ for ash with } \text{MMD}_i < 5 \mu\text{m} \end{aligned}$$

where

$$\begin{aligned} \text{MMD}_p &= \text{the MMD of the size distribution emerging from a very efficient collecting zone} \\ \text{MMD}_r &= \text{the MMD of the size distribution of rapped/reentrained material.} \end{aligned}$$

Step 8 – Use or compute the following factors for pure air:

$$\begin{aligned} \epsilon_0 &= 8.845 \times 10^{-12} \text{ free space permittivity (F/m)} \\ \eta &= 1.72 \times 10^{-5} (\text{Tk}/273)^{0.71} \text{ gas viscosity (kg/m-s)} \\ E_{bd} &= 630,000 (273/\text{Tk})^{1.65} \text{ electric field at sparking (V/m)} \\ \text{LF} &= S_N + \text{RR}(1 - S_N) \text{ loss factor (dimensionless)} \end{aligned}$$

For plate-wire ESPs:

$$\begin{aligned} E_{avg} &= E_{bd}/1.75 \text{ average field with no back corona} \\ E_{avg} &= 0.7 \times E_{bd}/1.75 \text{ average field with severe back corona} \end{aligned}$$

For flat plate ESPs:

$$\begin{aligned} E_{avg} &= E_{bd} \times 5/6.3 \text{ average field, no back corona, positive polarity} \\ E_{avg} &= 0.7 \times E_{bd} \times 5/6.3 \text{ average field, severe back corona, positive polarity} \end{aligned}$$

Step 9 – Assume the smallest number of sections for the ESP, n , such that $\text{LF}^n < p$. Suggested values of n are:

<u>Eff(%)</u>	<u>n</u>
<96.5	2
<99	3
<99.8	4
<99.9	5
>99.9	6

These values are for an LF of 0.185, corresponding to a coal fly ash precipitator. The values are approximate, but the best results are for the smallest allowable n .

Step 10 – Compute the average section penetration, p_s :

$$p_s = p^{1/n}$$

Step 11 – Compute the section collection penetration, p_c :

$$p_c = \frac{p_s - LF}{1 - LF}$$

If the value of n is too small, then this value will be negative and n must be increased.

Step 12 – Compute the particle size change factors, D and MMD_{rp} , which are constants used for computing the change of particle size from section to section:

$$\begin{aligned} D &= p_s = S_N + P_c(1 - S_N) + RR(1 - S_N)(1 - p_c) \\ &= MMD_{rp} = RR(1 - S_N)(1 - p_c)MMD_r / D \end{aligned}$$

Step 13 - Compute a table of particle sizes for sections 1 through n :

Section	MMD
1	$MMD_1 = MMD_i$
2	$MMD_2 = \{MMD_1 \times S_N + [(1 - p_c) \times MMD_p + p_c \times MMD_1] \times p_c\} / D + MMD_{rp}$
3	$MMD_3 = \{MMD_2 \times S_N + [(1 - p_c) \times MMD_p + p_c \times MMD_2] \times p_c\} / D + MMD_{rp}$
⋮	⋮
n	$MMD_n = \{MMD_{n-1} \times S_N + [(1 - p_c) \times MMD_p + p_c \times MMD_{n-1}] \times p_c\} / D + MMD_{rp}$